Article ID：1007−7294(2026)06−0910−15

Tensile and Relaxation Tests and Properties Studies of Polymer Materials for Marine Flexible Pipes

CHEN Kun−peng[1,2,3], *ZHANG Meng−meng*[3], *FU Shi−xiao*[3], *CHEN Te*[4], *DU Chang−jiang*[3]

(1. School of Mechanical Engineering, Quzhou University, Quzhou 324000, China; 2. Zhejiang Key Laboratory of Intelligent Manufacturing for Aerodynamic Equipment, Quzhou University, Quzhou 324000, China; 3. School of Ocean and Civil Engineering, Shanghai Jiao Tong University, Shanghai 200240, China; 4. Engineering Mechanics Experimental Center, Shanghai Jiao Tong University, Shanghai 200240, China)

Abstract: Polymer materials are usually applied to the sheath layers on the surface of marine flexible pipes. Such kind of material exhibits certain nonlinear characteristics, specifically manifested as a stress-strain nonlinearity and stress relaxation phenomena. In this paper, specimens are specially designed, and specific testing instruments are used according to relevant international standards to conduct tensile and stress relaxation tests on polymer materials for marine non-bonded pipes under high temperature environments. The tensile stress-strain curve and stress relaxation curve are obtained, and the Prony series constitutive parameters describing their stress relaxation characteristics are then identified from the stress relaxation test data, and verified using finite element method. Finally, the characteristics of stress relaxation in polymer materials are discussed. It is found that there is no pure elastic deformation stage in polymer materials during tensile deformation, and that the coexistence of elastic deformation and plastic deformation is reflected from the beginning of tensile deformation. The essence of stress relaxation phenomenon in polymer materials is the transformation from elastic to plastic deformation of the material. When plastic deformation accounts for the majority of internal deformation of the material, the percentage of stress reduction during the relaxation process will be smaller compared with the case when elastic deformation accounts for the majority. In engineering, if considering to reduce the effects of stress relaxation, polymer materials can be approximately taken as directly entering plastic deformation stage.

Key words: polymer materials; non-bonded flexible pipe; tensile test; high temperature stress relaxation test

CLC number: TB322 **Document code:** A **doi:** 10.3969/j.issn.1007−7294.2026.06.005

0 Introduction

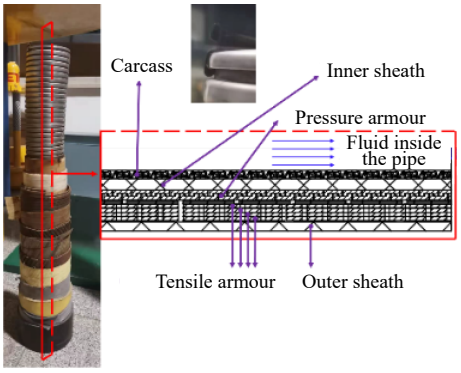
Polymer materials are commonly used to manufacture the sheath layers in the marine non-bonded flexible pipes, and the basic structural pattern of non-bonded pipes is shown in Fig.1. Due to the special structure of carcass, the inner surface will directly contact the internal fluid of the pipe. The sheath layer

Received date：2025−06−27

Foundation items：Supported by the National Key R&D Program of China (2023YFC2811600); the National Natural Science Foundation of China (52088102) and Fundamental Research Funds for the Central Universities (22X010201787)

Biography：CHEN Kun-peng(1995−), male, Ph.D., candidate; ZHANG Meng-meng(1991−), female, Ph.D., associate professor, corresponding author, E-mail: claire_zhang@sjtu.edu.cn.

contacts the metal ring in the end fittings to resist the leakage of internal fluid, and the basic form of the end sealing structure is shown in Fig.2. In practical engineering, in order to reduce transportation costs, the temperature of the internal fluid will be raised, which will cause severe stress relaxation of polymer materials, thereby affecting the sealing effect at the ends.



Flexible pipe axial section

Fig.1 Basic structure of non-bonded pipe

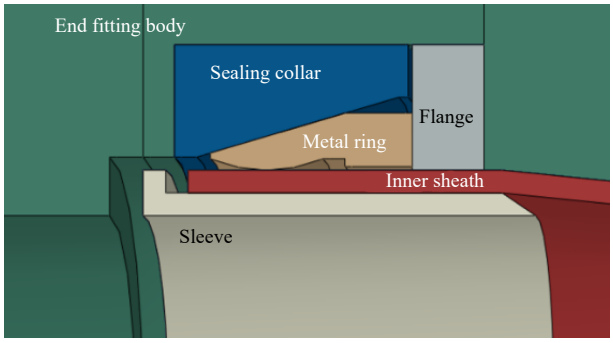


Fig.2 Basic structure of end sealing system

Gao et al[1−2] conducted biaxial tests on different membrane materials under different stress ratios to describe their nonlinear mechanical behavior in the form of polynomials. Ambroziak et al[3−5] completed tests on polyester-coated fabric membrane material under different conditions to discuss the nonlinear behavior of its mechanics and to propose a method for calculating material parameters. Penava et al[6] implemented tensile tests on anisotropic fabric materials to discuss the changing law of elastic modulus with tensile deformation, and finally concluded the relationship between elastic modulus and tensile angle. Han et al[7] and Falca et al[8] discussed the changes in mechanical properties of PVDF materials when they underwent modification. In these tests, the stress-strain relationships of different polymer materials show strong nonlinear characteristics, and change with the different internal compositions of the material, so it is difficult to summarize the universal modulus of elasticity and other material parameters. Therefore, in actual engineering projects, for the purpose of ensuring the accuracy of design and calibration, it is necessary to carry out the tensile test of polymer materials of the same batch of raw materials beforehand to obtain accurate tensile curves.

Hyper-elastic model and viscoelastic model are commonly used to describe the stress relaxation behavior of polymer materials. Yeoh[9] proposed a hyper-elastic model to describe the stress relaxation behavior of rubber materials and gave the corresponding parameters. The application of viscoelastic model can be traced back to 1992. Johnson et al[10] analyzed the step strain of rubber materials and first used the viscoelastic model to describe the phenomenon. In 2000, NASA's Tzikang[11] proposed a constitutive relationship about the viscoelasticity of materials in the form of the Prony parameter. Since then, the use of viscoelastic constitutive relationship to describe the stress relaxation behavior of materials has gradually become the mainstream of industry. Xiao et al[12] proposed a viscoelastic model to describe the stress relaxation behavior of rubber materials. Dong et al[13] carried out sealing tests on a rubber material and verified the accuracy of this constitutive relationship by using the nonlinear finite element software ABAQUS.

In this paper, the tensile test procedure of four polymer materials is designed according to the international standards, and the stress-strain curves of the specimens are measured. Then the tensile test data is processed to obtain the Young's modulus of the materials in the initial deformation stage and the tangent moduli at different deformations. At the same time, deformation characteristics of the materials in the process of stretching are discussed. Finally, this paper presents the performance of high temperature stress relaxation

tests of PA11 and PVDF, measurement of the relaxation curves, identification of the Prony parameters describing their stress relaxation characteristics, discussion of the behavioral characteristics of stress relaxation, and suggestions to reduce the effects of stress relaxation.

1 Test design

1.1 Testing specimens and apparatus

The raw material used for manufacturing the specimens is in the form of cylindrical tube as shown in Fig.3. According to the requirements of the international standard ASTM D638, the specimen should be in the shape of dog-bone and the thickness should be between 1.0 mm and 14.0 mm. In order to ensure that the specimen is not curved in both the length and width directions, the thickness of the specimen should not be too large. The thickness of the specimen is 2.5 mm. The geometry of the specimen is shown in Fig.4.



Fig.3 Raw materials for the specimen

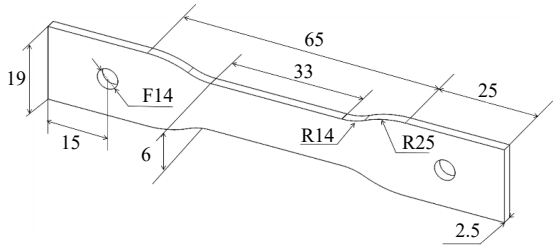


Fig.4 Geometric dimensions of the specimen

Both ASTM D638 and ASTM D2991 state that the tensile and relaxation properties of polymer materials are related to conditions such as tensile rate, temperature and other environment conditions during testing. Therefore, in this paper, the MTS universal testing machine in Shanghai Jiao Tong University Engineering Mechanics Test Center is used for the test, which has been verified by the relevant international standards. The tensile machine has a stroke of ±25 mm, a static loading capacity of ±2000 N, a dynamic loading capacity of ±3000 N and 1 high temperature reactor controlled by two groups of thermocouples. The basic structure of this stretching machine is shown in Fig.5, and the specimen mounted on the machine is shown in Fig.6. For this test, an extensometer with 25 mm pitch is used to measure the tensile displacement of the pitch section to calculate its strain.

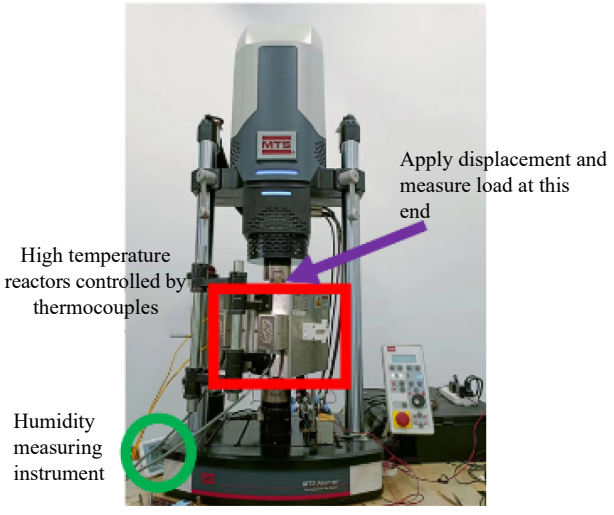


Fig.5 Basic composition of MTS stretching machine

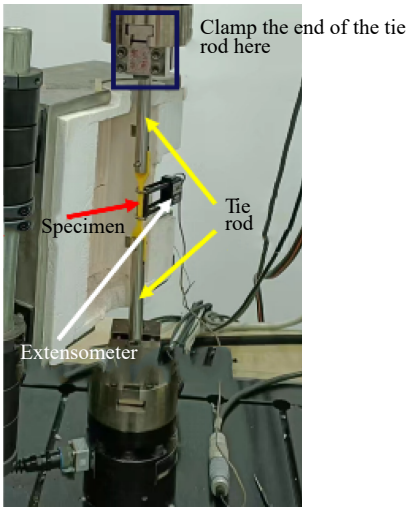


Fig.6 Installation form of the specimen

1.2 Test procedures and load cases

In this paper, four kinds of polymer materials provided by the producer: PA11, PVDF, PEX-B, and HDPE are firstly subjected to tension at ambient temperature. According to the test requirements of ASTM D638, the tensile test procedure is as follows: Firstly, the specimen is installed on the testing machine as shown in Fig.6; Secondly, the three-quarter force gauge measuring the force load is zeroed; Then, the specimen is stretched at a speed of 4 mm/min and the specimen status is recorded with the force-displacement graph on the monitor. When the force load decreases rapidly, it indicates that the specimen has partially failed and the stretching can be stopped. The maximum displacement that can be measured is 12.5 mm, which corresponds to 50% of the nominal strain. For most polymer materials, the specimen will partially fail before reaching this nominal strain value, so the measuring range of extensometer is enough.

After the tensile testing, PA11 and PVDF materials for stress relaxation tests under high temperature conditions are selected. The reason for choosing these two materials is that in the flexible pipes, they are usually used for the inner sheath, and this structure is often required to directly contact the high-temperature fluid transported inside the flexible pipe, where the stress relaxation phenomenon is more serious. The 18 loading cases for stress relaxation are shown in Tab.1.

Tab.1 18 load cases for high-temperature stress relaxation experiments

Case number	Material	Pre-strain	Temperature/℃	Case number	Material	Pre-strain	Temperature/℃
1	PVDF	1%	75	10	PVDF	15%	75
2	PVDF	1%	85	11	PVDF	15%	85
3	PVDF	1%	95	12	PVDF	15%	95
4	PVDF	2.5%	75	13	PA11	15%	75
5	PVDF	2.5%	85	14	PA11	15%	85
6	PVDF	2.5%	95	15	PA11	15%	95
7	PVDF	10%	75	16	PA11	30%	75
8	PVDF	10%	85	17	PA11	30%	85
9	PVDF	10%	95	18	PA11	30%	95

The testing procedure for stress relaxation is: (1) The specimen is mounted on the tensile machine where the high-temperature reactor is arranged. Considering that a certain gap will exist between the temperature of thermocouple and the specimen, it is necessary to utilize adhesive tape to attach the temperature sensor to the specimen; (2) The high-temperature reactor should be installed; (3) The thermocouple should be controlled to raise the temperature at a uniform rate so that the temperature of specimen reaches a preset temperature and maintains for 3 hours; (4) The specimen should be stretched to the pre-strain position at a speed of 2.5 mm/min and the indications of the triptych start to be recorded, every 10 s until after 24 h.

1.3 Stress relaxation curves and constitutive parameter identification method

The curve used to describe the relaxation behavior is called stress relaxation curve, and its horizontal axis is time, while the vertical axis is the axial load, the stress in material, or the relaxation modulus of material. The classical form of the relaxation curve is shown in Fig.7.

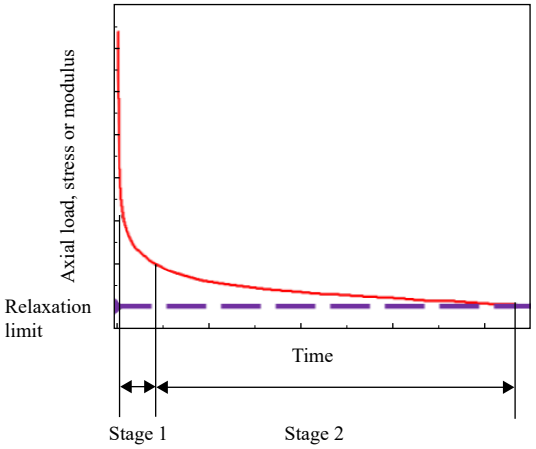


Fig.7 Classical form of relaxation curves

The relaxation modulus is defined as

$$E(t)=\frac{\sigma(t)}{\varepsilon} \tag{1}$$

where σ (t) is the value of the stress in the material at any point in time; ε is the fixed strain when stress relaxation occurs in a material.

The Prony parameter, commonly used to describe stress relaxation phenomena, has two forms

$$\begin{cases} E(t)=E_0\left[1-\sum_{i=1}^{j}g_i\left(1-\mathrm{e}^{-\frac{t}{\tau_i}}\right)\right], g_i>0, \tau_i>0, \sum_{i=1}^{j}g_i<1 & \text{(Method 1)} \\ E(t)=E_\infty+\sum_{i=1}^{j}E_i\mathrm{e}^{-\frac{t}{\tau_i}} & \text{(Method 2)} \end{cases} \tag{2}$$

where E_0 is the relaxation modulus of the material at the beginning of relaxation, i.e., at $t=0$; g_i, τ_i are Prony series describing the relaxation, which have j orders; E_∞ is the relaxation modulus of a material at its relaxation limit. In order to facilitate the discussion of the mechanical characterization of stress relaxation using the normalization method later on, Method 1 is chosen to characterize the stress relaxation curves.

In this paper, the axial force load-time curve $F(t)$−t can be obtained from the stress relaxation test. Then, according to the relationship between the axial force load F and the stress σ, the testing data is processed to obtain the nominal stress-time curve $\sigma(t)$−t. Finally, by Eq.(1), the relaxation modulus-time curve $E(t)$−t is obtained.

The program of its own is writtern in this paper to identify the Prony parameters in Method 1 shown in Eq.(2) from the relaxation modulus-time data points using the L-M method of nonlinear regression, and the program architecture is shown in Fig.8.

2 Results and discussions

2.1 Tensile curves and moduli of polymer materials

In this paper, tensile tests of four polymer materials at ambient temperature have been carried out, the four materials are: PA11, PVDF, PEX-B and HDPE. Two specimens of each material have been tested, and the results are shown in Fig.9.

From Fig.9, it can be seen that the stress-strain curves of each polymer material have a good coincidence, which indicates that the experimental procedure designed in this paper is valid and reliable. Meanwhile, it can be found from Fig.9 that all the stress-strain curves of the four polymer materials show significant nonlinear characteristics, with no completely linear phase in the curve, which indicates that no purely elastic phase exists in the stretching process of the polymer materials. This means that elastic deformation and plastic deformation always exist simultaneously in the specimen during its deformation. That is:

$$\varepsilon_{\text{total}}=\varepsilon_{\text{elastic}}+\varepsilon_{\text{plastic}} \tag{3}$$

It can be assumed that when the stress increases with the increase of strain, elastic deformation dominates the interior of the material. When the stress no longer increases or even decreases with strain, the internal plastic deformation increases. Fig.9 shows a rough estimate of the critical strain values for these four materials where elastic or plastic deformation is the dominant component within the material. These data are listed in Tab.2.

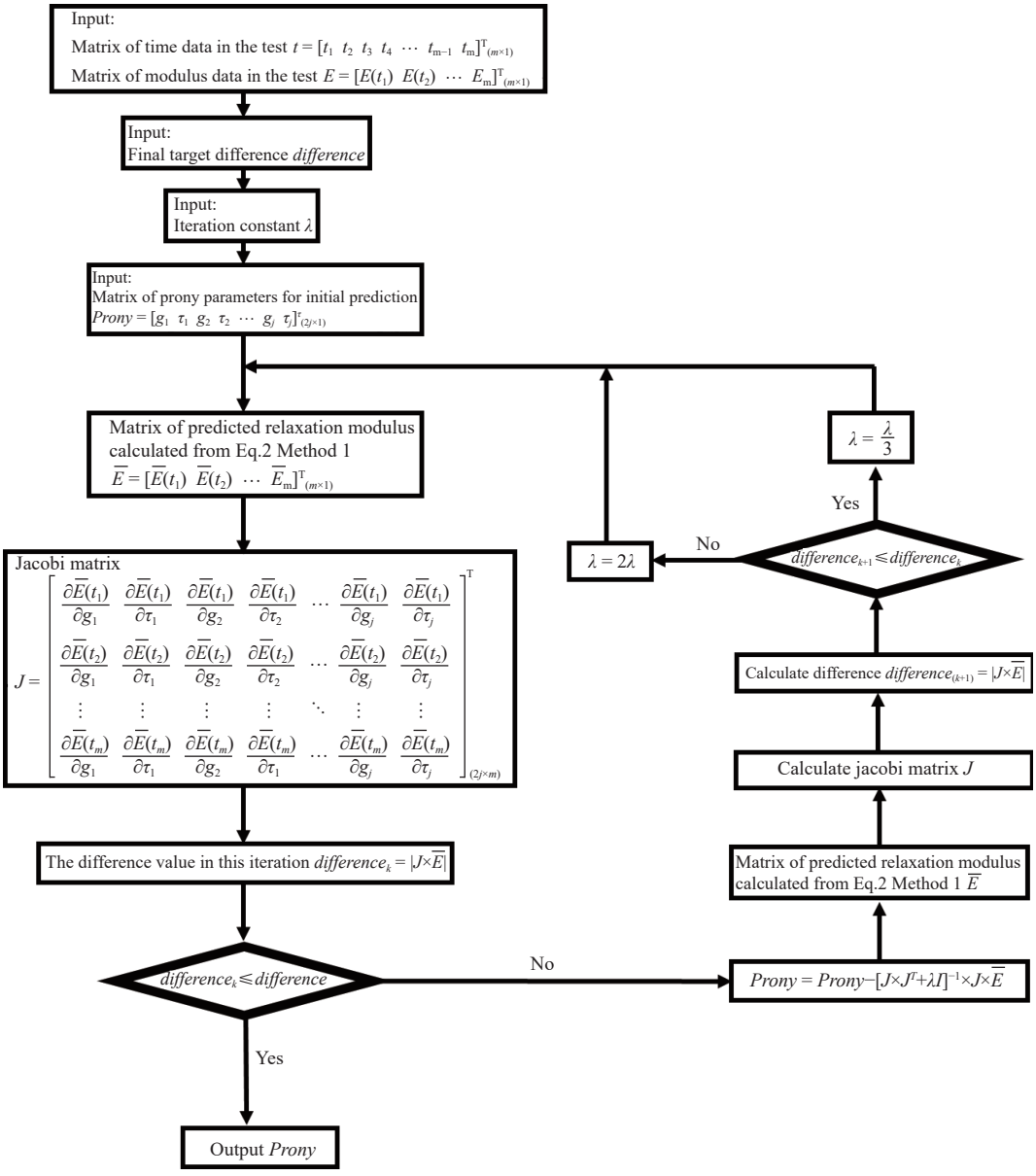
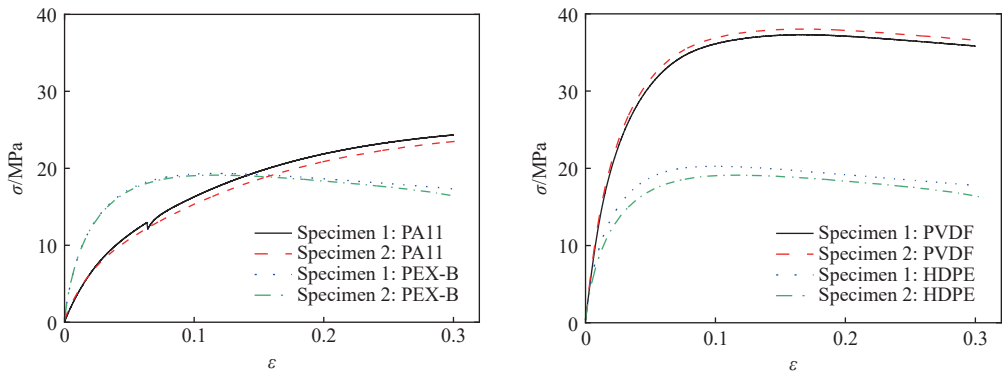


Fig.8 Procedure architecture of L-M nonlinear regression method



(a) PA11 and PEX-B　　(b) PVDF and HDPE

Fig.9 Stress-strain curves of four different polymer materials with different specimens

The data of the stress-strain curves are processed. Firstly, the data at the initial stage of the stress-strain curve which can be considered as a linear stage are selected for linear regression to obtain the so-called "linear stage modulus of elasticity". Then the tangent moduli at different strains are calculated, and the yield strength is obtained. These data are shown in Tab.3.

Tab.2 Critical strain for the predominance of elastic or plastic deformation within four polymer materials

Type of material	PA 11	PVDF	PEX-B	HDPE
Critical strain values	≥30%	About 7%~8%	About 5%	About 6%

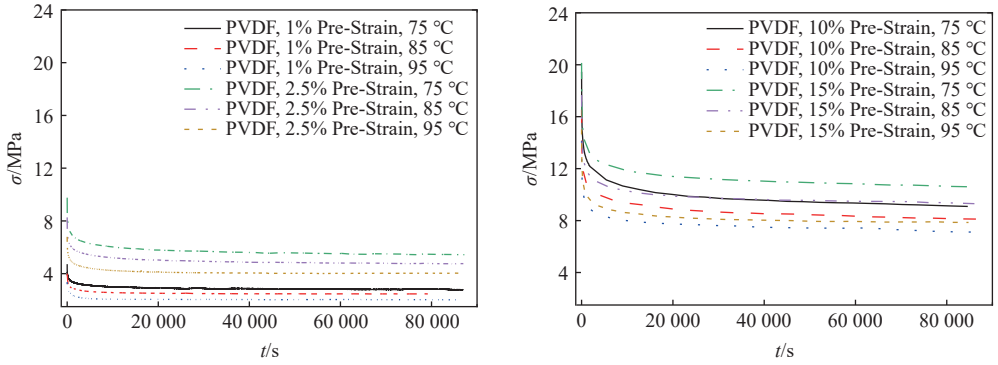
Tab.3 Data processing results for "nominal stress-strain" curves

Material	Project	Linear stage	Linear stage modulus of elasticity/MPa	Cut-line modulus of 10% strain/MPa	Cut-line modulus of 20% strain/MPa	Cut-line modulus of 30% strain/MPa	Yield strength/MPa
PA11	Specimen 1	-	-	162.79	109.39	81.11	-
PA11	Specimen 2	-	-	152.97	104.41	78.25	-
PA11	Average	-	-	157.88	106.90	79.68	-
PVDF	Specimen 1	0~3.27%	1466.85	361.29	185.54	119.50	34.96
PVDF	Specimen 2	0~3.27%	816.21	368.83	189.36	121.98	35.40
PVDF	Average	0~3.27%	1141.53	365.06	187.45	120.74	35.18
PEX-B	Specimen 1	0~1.07%	809.31	192.50	93.14	57.80	19.35
PEX-B	Specimen 2	0~1.07%	1575.59	190.32	91.77	54.69	19.13
PEX-B	Average	0~1.07%	1192.45	191.41	92.46	56.25	19.24
HDPE	Specimen 1	0~2.31%	1506.97	202.53	95.82	59.26	20.30
HDPE	Specimen 2	0~2.31%	625.28	202.16	95.82	59.26	20.30
HDPE	Average	0~2.31%	1066.13	202.16	95.82	59.26	20.30

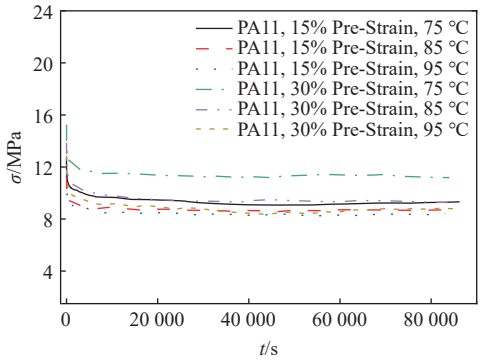
From the data in Tab.3, it can be seen that the difference in the "Linear Stage Modulus of Elasticity" of all the materials is very large. The reason is that the selection of the linear stage is too long. However, in practical engineering applications, strain of the material often exceeds this range, and the value of elastic modulus estimated by using these linear stages will lead to a large difference in results of mechanical analysis. Therefore, in practical engineering applications, it is recommended to estimate the deformation of the material beforehand, and then use the stress-strain curve tangent modulus under the corresponding strain as the basis for design and calibration.

2.2 Stress relaxation curves of polymeric materials and 3rd-order Prony parameters

The high-temperature stress relaxation testing conditions in this paper are shown in Tab.1, and the test results are expressed in the form of relaxation curves with time as the horizontal coordinate and stress as the vertical coordinate. The stress-time curves are given in Fig.10. The 3rd-order Prony parameters obtained by the identification method in Section 1.3 are presented in Tab.4.



(a) Load cases 1-6 (b) Load cases 7-12



(c) Load cases 13-18

Fig.10 Stress-time curve under 18 load cases

Tab.4 3rd-order Prony parameters describing the stress-time curve

Load case	Material	Pre-strain	Temperature/℃	g_1	τ_1	g_2	τ_2	g_3	τ_3
1	PVDF	1%	75	0.2000	37.9575	0.1207	1149.5660	0.0825	14 560.7399
2	PVDF	1%	85	0.1914	45.6856	0.1252	1236.1081	0.0664	10 894.3307
3	PVDF	1%	95	0.1593	41.8456	0.2127	1267.0072	0.0246	13 313.5965
4	PVDF	2.5%	75	0.2075	51.7376	0.1336	1348.7415	0.0993	19 529.7482
5	PVDF	2.5%	85	0.1964	56.9105	0.1329	1376.3227	0.0936	18 614.0205
6	PVDF	2.5%	95	0.1657	47.2842	0.1392	784.1672	0.1010	8572.5226
7	PVDF	10%	75	0.1824	18.6452	0.1674	360.9211	0.1753	11 329.1418
8	PVDF	10%	85	0.1861	21.9327	0.1684	390.1632	0.1492	13 351.8952
9	PVDF	10%	95	0.1784	22.3243	0.1764	385.4812	0.1298	11 555.1382
10	PVDF	15%	75	0.1656	20.8528	0.1707	414.2844	0.1271	13 999.7815
11	PVDF	15%	85	0.1607	20.9726	0.1781	397.6994	0.1226	9959.3846
12	PVDF	15%	95	0.1652	22.8580	0.1806	444.3544	0.1225	9413.6908
13	PA11	15%	75	0.0892	14.9319	0.0835	349.3940	0.0988	9038.0130
14	PA11	15%	85	0.0807	16.4951	0.0918	257.6714	0.0570	5935.6576
15	PA11	15%	95	0.0801	16.4093	0.1049	251.1003	0.0782	5884.0841
16	PA11	30%	75	0.1133	20.8594	0.0847	363.1189	0.0602	5466.6151
17	PA11	30%	85	0.1113	19.3623	0.1003	318.7693	0.1127	6818.6139
18	PA11	30%	95	0.1094	13.2271	0.1168	278.1541	0.1019	10 019.3560

It is worth noting that the 3rd-order Prony parameters obtained in Tab.4 are not unique with respect to the initial input forecasting matrix Prony and the target difference shown in the block diagram of the program in Fig.8.

2.3 Finite element verification of Prony parameters

The viscoelastic materials module in the nonlinear finite element software ABAQUS describes the stress relaxation behavior of the material using Method 1 in Eq.(2). Therefore, for the purpose of verifying the Prony parameters in Tab.4, ABAQUS software is used to establish the finite element model of the specimen part within the extensometer. The model is a cuboid with a section of 6 mm×2.5 mm and a length of 25 mm. In the calculation, the 6 degrees of freedom of one boundary of the model are all fixed, and the other boundary is controlled by displacement, so that the model reaches the predetermined strain. When the specimen generates the predetermined strain, the analysing step is set as the viscoelastic analysis step, and two boundaries of the model are fixed at the current positions, and the calculation time is 90 000 s.

However, the model in ABAQUS is three-dimensional, which will produce "shape effect" and

"boundary effect", as shown in Fig.11, so the stress of each node on the cross-section will be different due to the location and distance between itself and the boundary, and thus it is difficult to find a node whose stresses can represent the average stress of the cross-section. To solve this problem, a reference point is inserted on the free boundary section and the reference point is coupled with the free boundary section, as shown in Fig.12.

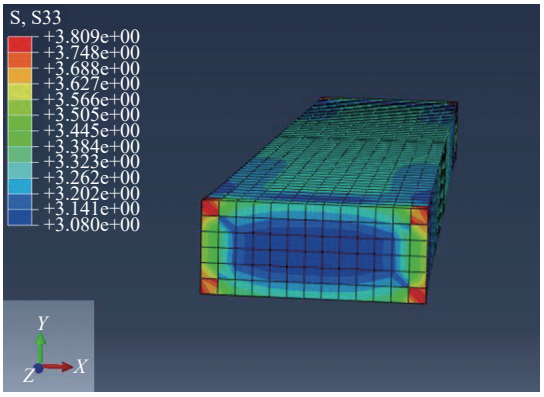


Fig.11 Stress diagram of different nodes on the boundary section

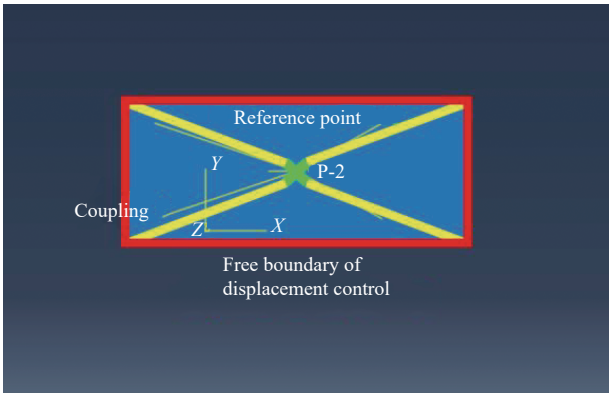
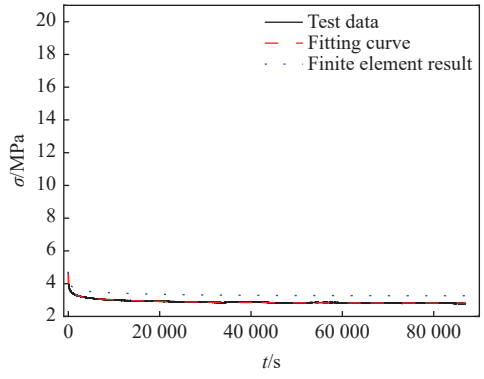
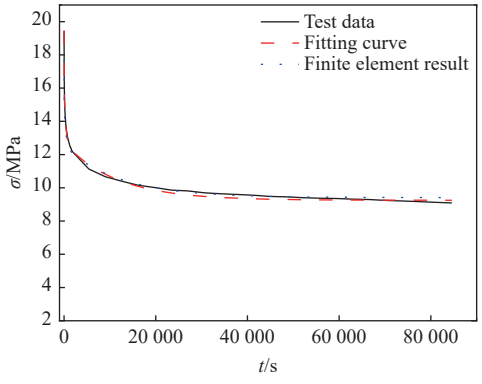


Fig.12 Schematic diagram of insertion reference points and their coupling to cross sections

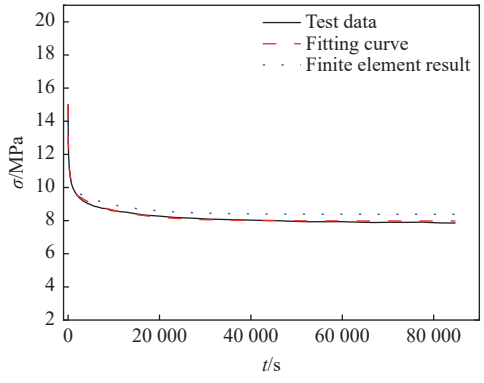
After the calculation, the reaction force (RF3) of the reference point is extracted, and the value of reaction force is divided by the cross-sectional area to obtain the average stress on the cross section. The Prony parameters in Tab.4 is then used to fit the stress curve for comparison with the finite element results and test data. Due to the large amount of cases, Fig.13 only samples the comparison curves for Cases 1, 7, 12, and 18, and the comparison curves for the remaining cases can be found in Appendix A.



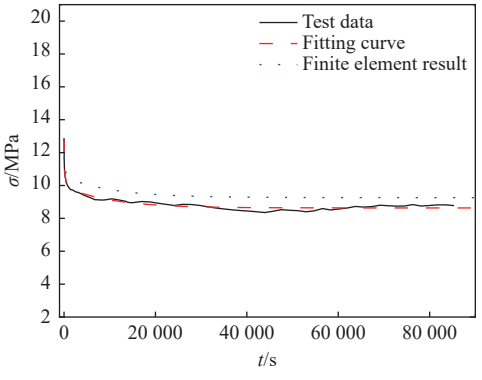
(a) Load Case 1



(b) Load Case 7



(c) Load Case 12



(d) Load Case 18

Fig.13 Comparison of test data, fitting curves and finite element results

As can be seen from Fig.13 and Appendix A, the three curves for each load case have good consistence, and the final relaxation limits do not differ by more than 1 MPa, which indicates that the stress relaxation constitutive model in the form of Prony parameters chosen in this paper can accurately describe the stress relaxation behavior, and the parameter identification program established in this paper can identify the Prony parameters in the constitutive model with the experimental data.

The reason for the difference between finite element result and testing data in relaxation limit for each case is that, in the test, the cross-section of the specimen's pitch section does not have deformation constraints in both the width and thickness directions (x, y-axis directions in Fig.11 and Fig.12), but the cross section coupled with reference point in the finite element model makes constraints in these two directions. When the test data are processed, the stress relaxation is considered to occur only in the tensile direction of the specimen, and the stress σ is obtained by dividing the force F at each moment by the cross-sectional area of the specimen A (6 mm×2.5 mm), and the relaxation modulus E is obtained by dividing the stress σ by a fixed strain ε. These data are applicable only to the dimension of the tensile direction (z-axis direction in Fig.11 and Fig.12), and changes in both the width and thickness directions of the cross-section are ignored. In the simulation calculation of ABAQUS software, the model of the specimen is three-dimensional, in addition to the stress relaxation phenomenon in the tensile direction of the specimen, the stress relaxation phenomenon also exists in the other two directions of the specimen. In the simulation process, when stress relaxation occurs in the other two directions of the specimen (x, y-axis directions in Fig.11 and Fig.12), there is a tendency of shortening the specimen in the axial direction (z direction) and reducing the cross-sectional area under the influence of the shape effect. In the stress relaxation process simulated by finite element, in order to ensure that the elongation of the specimen can always meet the requirements of the material to generate pre-strain, the cross-section coupled with reference point in Fig.12 is fixed throughout the entire process at the position after the displacement occurs, and no point on the cross-section is allowed to generate any displacement in the degrees of freedom, which leads the reference point to bear an additional support reaction force (RF3) to resist the tendency of axial shortening and reduction of cross-sectional area. Therefore, the stress results obtained by dividing the branch reaction force data by the cross-sectional area in the extracted finite element simulation results in this paper will be slightly larger than the test results. This is the reason that the relaxation limit of "Finite Element Result" is slightly larger than those of the other two curves in the three curves of 18 load cases.

2.4 Discussion of relaxation properties based on relaxation modulus normalization

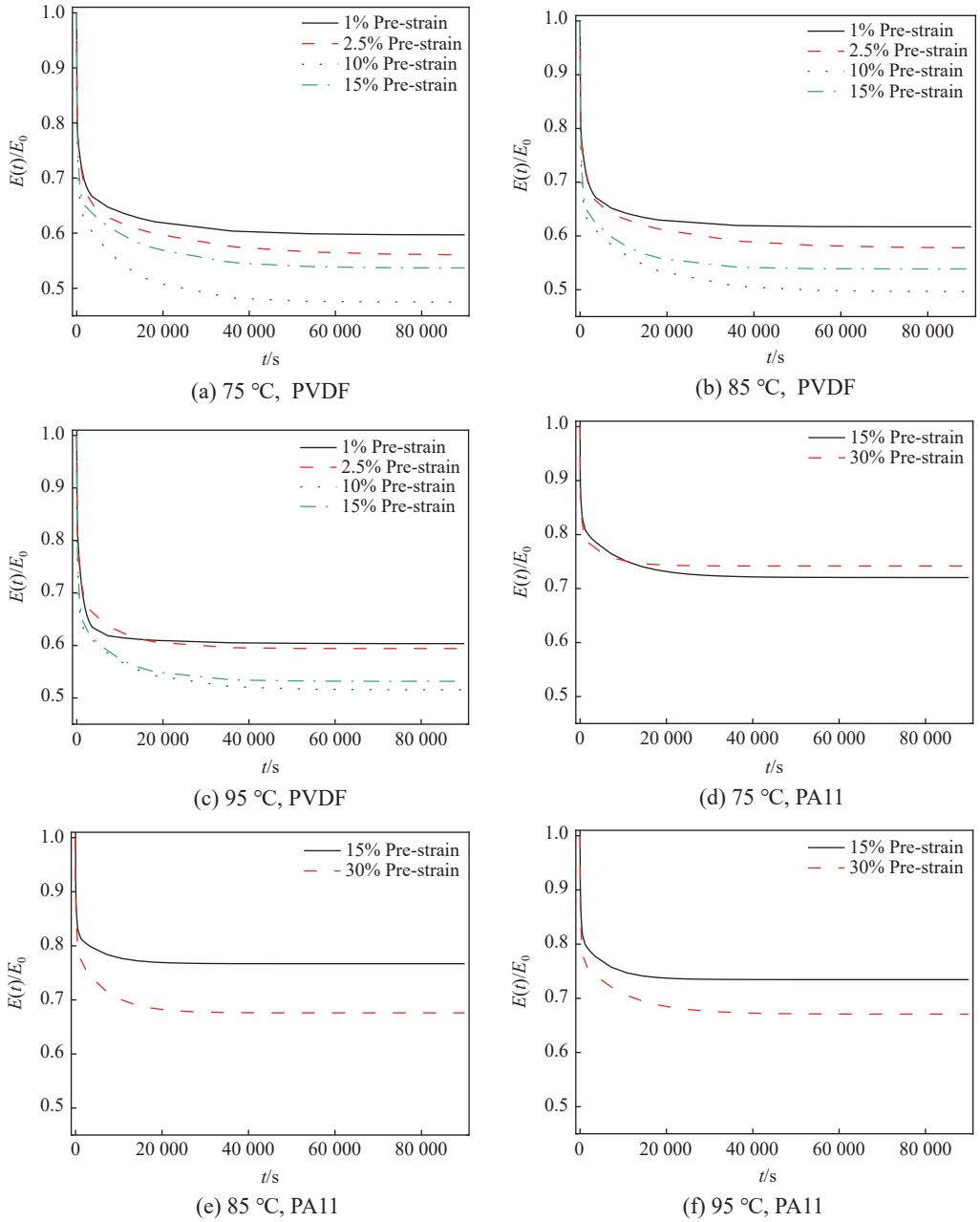
In order to further discuss the mechanical properties of the material during stress relaxation, the relaxation modulus during relaxation is normalized using the fitted 3rd-order Prony parameter

$$E(t)/E_0 = 1 - \sum_{i=1}^{3} g_i \left(1 - \mathrm{e}^{-\frac{t}{\tau_i}}\right) \tag{4}$$

Fig.14 gives the normalized relaxation modulus curves for PVDF and PA11 materials at the same temperature and different pre-strain, respectively.

From Fig.14(a)−(c), it can be seen that the decrease in relaxation modulus of PVDF specimens during stress relaxation is in the following order from the smallest to the largest under the same temperature conditions: 1% pre-strain < 2.5% pre-strain < 15% pre-strain < 10% pre-strain. Reviewing the data given in Tab.2, at 10% nominal strain and above, plastic deformation has slowly begun to possess a greater share of the overall deformation of the specimen. It is generally accepted that the stress relaxation phenomenon in material is the conversion of a portion of the elastic strain to plastic strain on the premise that the overall strain in material remains unchanged. When the overall deformation of the material is dominated by elastic

deformation, the material has a sufficiently large base of elastic deformation that can be converted to plastic deformation. As the proportion of plastic deformation increases in the overall deformation of the material before relaxation, the base of elastic deformation that can be converted to plastic deformation in the material becomes smaller, and thus the decrease in modulus during relaxation becomes smaller. For the above reason, number of relaxation modulus decreases for the "15% pre-strain" curve < that for the "10% pre-strain" curve.



(a) 75 ℃, PVDF (b) 85 ℃, PVDF

(c) 95 ℃, PVDF (d) 75 ℃, PA11

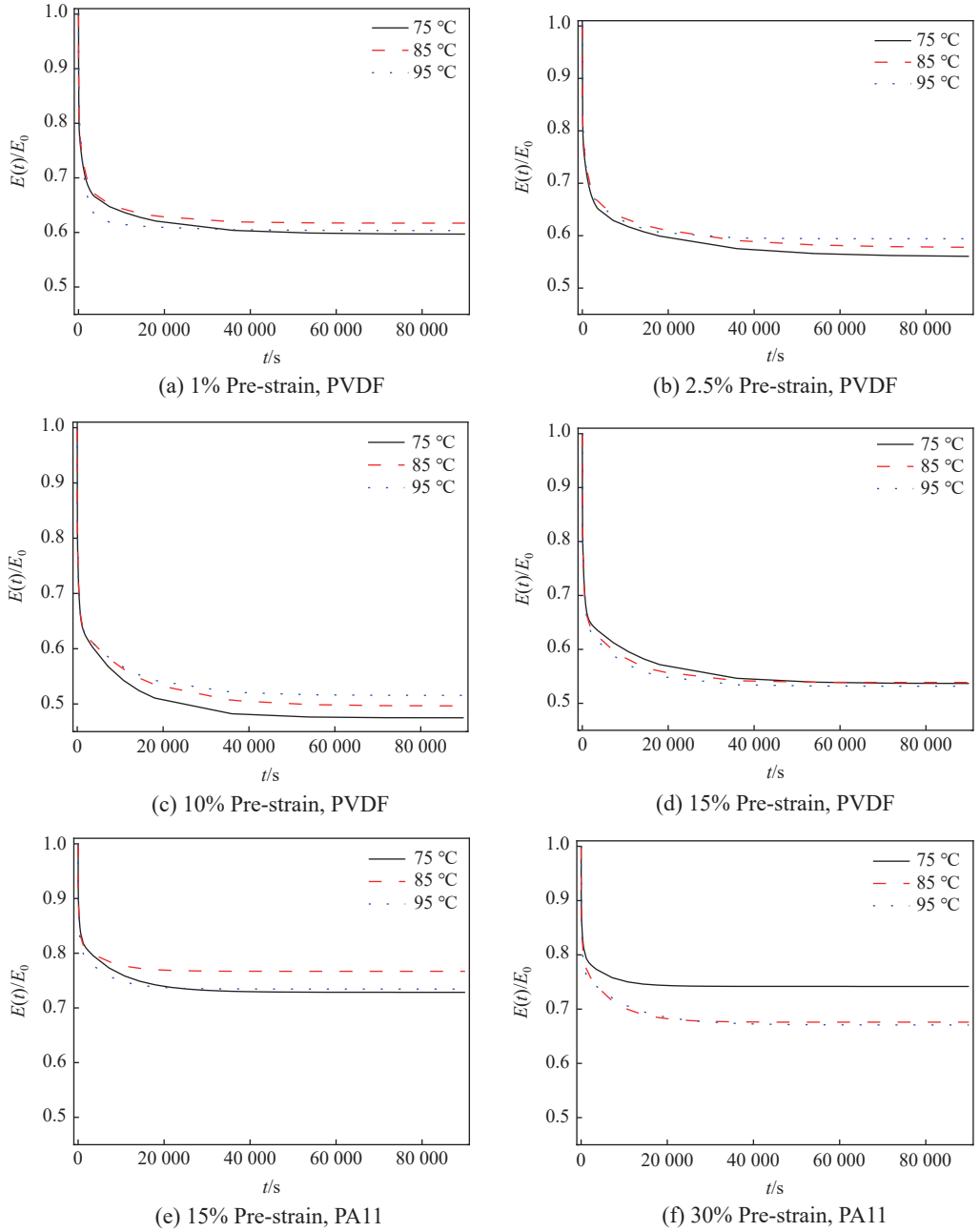
(e) 85 ℃, PA11 (f) 95 ℃, PA11

Fig.14 Normalized relaxation modulus curves of PVDF and PA11 under different pre-strains at the same temperature

Observing the nominal stress curve of the PVDF specimens in Fig.9(b), it is not difficult to find that the material can take up a larger stress at 15% strain than at 1% strain and 2.5% strain. Consequently, when polymer materials are used in high temperature environments, if the method for reducing the effects caused by stress relaxation is considered solely, the strain of the polymer materials can be appropriately increased to a larger proportion of their internal plastic deformation.

However, the PA11 materials show a different pattern at 75 ℃: the decrease of relaxation modulus has:

15% pre-strain > 30% pre-strain, which may indicate that the relaxation phenomenon of PA11 materials is not significant at 75 ℃. Fig.15 gives the normalized relaxation modulus curves of these two materials at different external temperatures under the same pre-strain conditions.



(a) 1% Pre-strain, PVDF　　(b) 2.5% Pre-strain, PVDF

(c) 10% Pre-strain, PVDF　　(d) 15% Pre-strain, PVDF

(e) 15% Pre-strain, PA11　　(f) 30% Pre-strain, PA11

Fig.15 Normalized relaxation modulus curves of PVDF and PA11 material at different temperatures under the same pre-strain

As can be seen in Fig.15(a)−Fig.15(d), the relaxation of PVDF materials at external temperatures of 75 ℃, 85 ℃ and 95 ℃ are similar. Observing Fig.15(f), the two curves at 85 ℃ and 95 ℃ show a significant increase in relaxation amplitude compared to the 75 ℃ curve, whereas this phenomenon is not obvious in Fig.15(e). This may indicate that the stress relaxation properties of PA11 are less sensitive to temperature at 15% pre-strain, while the temperature sensitivity of the stress relaxation properties of PA11 is stronger when the value of strain reaches 30%, which makes the relaxation amplitude of the material at 75 ℃ much smaller than those at 85 ℃ and 95 ℃. From the data in Tab.2, it can be seen that no matter 15% strain or 30% strain,

the elastic strain inside PA11 is dominant, and at temperatures of 85 ℃ and 95 ℃, which are with larger relaxation sensitivity, it still conforms to the law that the larger the percentage of elastic deformation inside the specimen is, the larger the relaxation amplitude will be.

3 Conclusions

This paper conducted tensile tests of four kinds of polymer materials according to the international standards to obtain the stress-strain curve, and then investigated the basic mechanical characteristics of polymer materials based on these curves. After that, this paper accomplished stress relaxation tests under high-temperature conditions for PA11 and PVDF to obtain the relaxation curves under different load cases, from which the 3rd-order Prony parameters describing the stress relaxation curves were identified, and then the characteristics of stress relaxation phenomenon and effects of the external environment on the stress relaxation were both analysed. The conclusions of this paper are as follows:

(1) The stress-strain curves of four kinds of polymer materials show strong nonlinear characteristics when they are subjected to stretching, which indicates that even if the deformation of the material is small, elastic deformation and plastic deformation exist in the material at the same time. As a result, it is difficult to obtain the modulus of elasticity from the linear deformation phase of the material. It is recommended that in the actual project the load or deformation to the materials should be estimated in advance, and then the tangent modulus of stress-strain curve from material tests could be used as a material parameter for design and verification.

(2) The essence of stress relaxation phenomenon is that a part of the elastic strain inside the material transforms into plastic strain while the overall strain remains unchanged. Therefore, if the external environment is the same, when the deformation inside the material is dominated by elastic deformation, the magnitude of stress relaxation will be greater than that when plastic deformation dominates inside the material. Therefore, in engineering applications, if the purpose is simply to reduce the influence of stress relaxation on structural safety, the polymer materials can be considered to enter the deformation stage dominated by plastic deformation.

(3) At 75 ℃, 85 ℃ and 95 ℃, the temperature has little effect on the relaxation amplitude of PVDF, which follows the law that the more the elastic deformation inside the material is, the larger the relaxation amplitude is. For PA11 materials, under 15% strain, the sensitivity of stress relaxation amplitude to temperature is low, and under 30% strain, the sensitivity of stress relaxation amplitude to temperature is high, basically following the law that the more elastic deformation inside the material is, the greater the relaxation amplitude is.

References

[1] Gao C, Chen W, Shi T, et al. Response surface characterization for biaxial tensile properties of envelope fabrics under multiple stress ratios[J]. Composite Structures, 2019, 230: 111482.

[2] Gao C, Chen W, Hu J, et al. A new constitutive model on biaxial tensile behavior of architectural fabrics[J]. Polymer Testing, 2020, 87: 106519.

[3] Ambroziak A, Klosowskl P. Mechanical testing of technical woven fabrics[J]. Journal of Reinforced Plastics and Composites, 2013, 32(10): 726−739.

[4] Ambroziak A, Klosowskl P. Mechanical properties for preliminary design of structures made from PVC coated fabric[J]. Construction and Building Materials, 2014, 50: 74−81.

[5] Ambroziak A. Mechanical properties of precontraint 1202s coated fabric under biaxial tensile test with different load ratios[J]. Construction & Building Materials, 2015, 80(Apr. 1): 210−224.

[6] Penava Z, Penava D S, Knezic Z. Determination of the elastic constants of plain woven fabrics by a tensile test in various directions[J]. Fibres & Textiles in Eastern Europe, 2014, 104(2): 57−63.
[7] Han K, Wang T, Zhang N, et al. A film coating assembled by tubular nitrogen-doped carbon fibers as an efficient membrane spacer to suppress the shuttle effect for long-life lithium-sulfur batteries[J]. Electrochimica Acta, 2021, 365: 137232.
[8] Falca G, Mustesta V E, Behzad A R, et al. Cellulose hollow fibers for organic resistant nanofiltration[J]. Journal of Membrane Science, 2019, 586: 151−161.
[9] Yeoh O H. Some forms of the strain energy function for rubber[J]. Rubber Chemistry and Technology, 1993, 66(5): 754−771.
[10] Johnson A R, Quigley C J. A viscohyperelastic maxwell model for rubber viscoelasticity[J]. Rubber Chem. Technol, 1992, 65(1): 137−153.
[11] Tzikang C. Determining a Prony series for a viscoelastic material from time varying strain data[R]. NASA Langley Technical Report Server. 2000.
[12] Xiao R, Sun H, Chen W. An equivalence between generalized maxwell model and fractional zener model[J]. Mechanics of Materials, 2016, 100: 148−153.
[13] Dong Y, Ke Y, Zheng Z, et al. Effect of stress relaxation on sealing performance of the fabric rubber seal[J]. Composites Science & Technology, 2017, 151: 291−301.

海洋非粘结管用高分子材料拉伸及应力松弛试验及其特性研究

陈鲲鹏[1,2,3]，张萌萌[3]，付世晓[3]，陈　特[4]，杜长江[3]

（1. 衢州学院机械工程学院，浙江 衢州，324000；2. 浙江省空气动力装备智能制造重点实验室，浙江 衢州，324000；3. 上海交通大学船舶海洋与建筑工程学院，上海 200240；4. 上海交通大学力学测试中心，上海 200240）

摘要：聚合物材料通常用于制造海洋柔性管中的护套层。聚合物材料在柔性管道系统的工作温度下表现出一定的非线性特性，具体表现为应力−应变非线性和应力松弛现象。本文根据相关国际规范设计试样、选择试验仪器，然后对海洋非粘结管用聚合物材料进行拉伸试验与高温环境下的应力松弛试验，获得拉伸应力应变曲线和应力松弛曲线，从应力松弛试验数据中辨识描述其应力松弛特性的 Prony 级数形式的本构参数，并利用有限元方法进行验证。最后，讨论聚合物材料应力松弛的特性。研究发现，聚合物材料在拉伸变形中无纯弹性变形阶段，从最开始便体现出弹性变形与塑性变形共存的特征；聚合物材料应力松弛现象的本质为材料内部的弹性变形向着塑性变形转化，当塑性变形占材料内部变形的主体时，其应力松弛过程中应力下降的百分比将会比弹性变形占主体时小；若单纯以减少应力松弛的不利影响考虑，可使聚合物材料适当进入塑性变形为主导的变形阶段。

关键词：聚合物材料；非粘结管道；拉伸试验；高温应力松弛试验

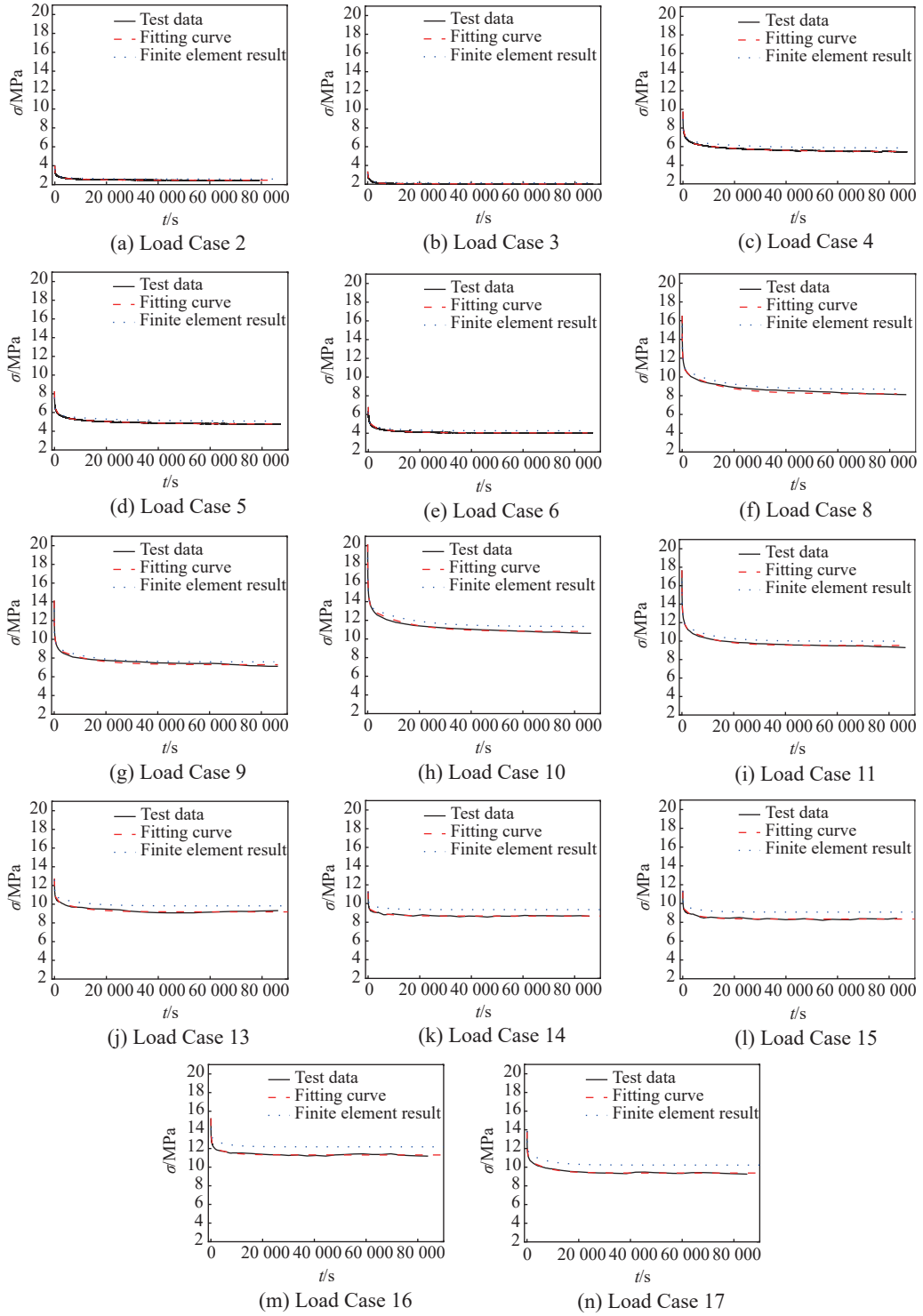
中图分类号：TB322　　**文献标识码：**A

基金项目：科技部重点研发计划青年科学家项目（2023YFC2811600）；国家自然科学基金基础科学中心项目（52088102）；中央高校基本科研业务费资助项目（22X010201787）

作者简介：陈鲲鹏（1995−），男，上海交通大学博士研究生；
张萌萌（1991−），女，上海交通大学副教授、博士生导师；
付世晓（1976−），男，上海交通大学教授、博士生导师；
陈　特（1991−），男，上海交通大学实验员；
杜长江（1999−），男，上海交通大学硕士研究生。

Appendix A:

Due to the limitation of space, Fig.13 in section 2.3 only shows the comparison of test data, fitting curves and finite element results of Load Cases 1, 7, 12 and 18, and the comparison diagrams of the remaining 14 load cases are shown in Fig.A-1.



(a) Load Case 2 (b) Load Case 3 (c) Load Case 4

(d) Load Case 5 (e) Load Case 6 (f) Load Case 8

(g) Load Case 9 (h) Load Case 10 (i) Load Case 11

(j) Load Case 13 (k) Load Case 14 (l) Load Case 15

(m) Load Case 16 (n) Load Case 17

Fig.A1 Comparison diagram of test data, fitting curve and finite element result